Self-Calibrating Indoor Trajectory Tracking System Using Distributed Monostatic Radars For Large Scale Deployment

Zongxing Xie
ECE Dept., Stony Brook University, USA
zongxing.xie@stonybrook.edu

Fan Ye
ECE Dept., Stony Brook University, USA
fan.ye@stonybrook.edu

ABSTRACT

24/7 continuous recording of in-home daily trajectories is informative for health status assessment (e.g., monitoring Alzheimer's, dementia based on behavior patterns). Indoor device-free localization/tracking are ideal because no user efforts on wearing devices are needed. However, prior work mainly focused on improving the localization accuracy. They relied on well-calibrated sensor placements, which require hours of intensive manual setup and respective expertise, feasible only at small scale and by mostly researchers themselves. Scaling the deployments to tens or hundreds of real homes, however, would incur prohibitive manual efforts, and become infeasible for layman users. We present *SCALING*, a plug-and-play indoor trajectory monitoring system that layman users can easily set up by walking a one-minute loop trajectory after placing radar nodes on walls. It uses a self calibrating algorithm that estimates sensor locations through their distance measurements to the person walking the trajectory, a trivial effort without taxing layman users physically or cognitively. We evaluate *SCALING* via simulations and two testbeds (in lab and home configurations of sizes 3×6 sq m and 4.5×8.5 sq m). Experimental results demonstrate that *SCALING* outperformed the baseline using the approximate multidimensional scaling (MDS, the most relevant method in the context of self calibration) by 3.5 m/1.6 m in 80-percentile error of self calibration and tracking, respectively. Notably, only 1% degradation in performance has been observed with *SCALING* compared to the classical multilateration with known sensor locations (anchors), which costs hours of intensive calibrating effort.

CCS CONCEPTS

• **Applied computing** → **Health informatics**; • **Human-centered computing** → **Ubiquitous and mobile computing systems and tools**.

KEYWORDS

Radio Frequency (RF) Sensing; Anchor-free; Indoor Tracking; Local Positioning System; Monostatic Radars; Distributed Radars

ACM Reference Format:
Zongxing Xie and Fan Ye. 2022. Self-Calibrating Indoor Trajectory Tracking System Using Distributed Monostatic Radars For Large Scale Deployment. In *The 9th ACM International Conference on Systems for Energy-Efficient Buildings, Cities, and Transportation (BuildSys '22), November 9–10, 2022, Boston, MA, USA.* ACM, New York, NY, USA, 10 pages. https://doi.org/10.1145/3563357.3564078

This work is supported in part by NSF grants 1951880, 2028952, 2119299.

BuildSys '22, November 9–10, 2022, Boston, MA, USA

ACM ISBN 978-1-4503-9890-9/22/11…$15.00
https://doi.org/10.1145/3563357.3564078

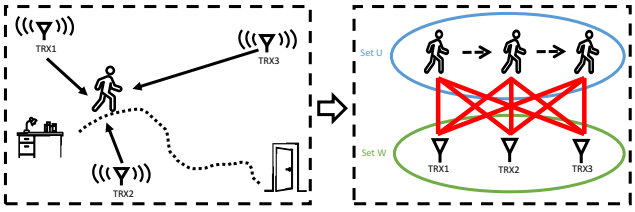

Figure 1: We present *SCALING* (Self-Calibrating Indoor Tracking), which uses distributed monostatic radars to measure distances to the human subject for multilateration thus tracking daily indoor trajectories, informative for health status assessment. We aim to save intensive efforts on calibrating sensor placements with a novel self calibrating algorithm which formulates the problem in a bipartite graph and obtain the uniqueness of geometrical topology according to the rigidity of graph. With that, the daily indoor trajectories can be extracted in this local positing system in the absence of anchors of known locations to be referenced.

1 INTRODUCTION

With rapid advancements in Internet of Things (IoT), in-home health monitoring systems are receiving increasing attention in our aging society with the goal of creating smart homes that support older adults to age in place. Among several types of monitoring data, users' daily indoor trajectories are invaluable for health status assessment. With that, we can extract the low-level information about how capable or how fast a user can ambulate from one place to another. We can further derive the high-level information, for example, the duration and the frequency of engagements in certain functional spaces, such as the bathroom. Such information provides insights about users' daily routines and behavior patterns, critical indicators not available from hospital visits (e.g., hesitant steps could indicate the onset or progression of Alzheimer's dementia).

Prior Work on Device-free Indoor Tracking and Scoping. Device-free schemes for indoor tracking are user-friendly because they do not require users to carry or wear any devices. Among typical categories, geophones or vibration sensors require costly refurbishment for large coverage [28, 30]; vision [18] or acoustic [16] based monitoring solutions are highly susceptible to background interferences (lighting conditions or background noises), and sometimes may incur privacy concerns. Recent efforts have shown preferable features of RF techniques [5], which are free of the aforementioned issues. People have explored localization/tracking using WiFi [24, 37], FMCW [2, 3], UWB [13, 41] based on proximity [9], fingerprinting [7], parameter joint estimation [32, 37], and triangulation (including trilateration and angulation) [24]. While such solutions were reported with promising results, they usually rely on well-calibrated sensor placements, which require hours of intensive manual setup and respective expertise, feasible only at small scale and by mostly researchers themselves. Scaling the deployments to tens or hundreds of real homes, however, would incur prohibitive manual efforts, and become infeasible for layman users. Some may argue that RF sensing systems with single-site

configurations [1–3] can be preinstalled and wrapped up in a compact box thus easy for scaling. However, their localization performance will degrade significantly when the subject is far away from the single-site sensor due to the fixed angle resolution [24], and coordinating their hand-off from one site to another remains an open challenge [2]. Therefore, we limit the scope of our paper to device-free indoor localization/tracking using distributed setups of multiple sensors, which by nature eliminate the hand-off concerns by consistent coverage thus localization performance no matter where the subject is located.

Design Considerations. With the above discussion, the costly sensor deployment effort for scaling remains as an issue to be solved. More specifically, the core challenge comes from the necessity of calibrating sensor placements with careful measurements and respective expertise. To address that, we present a plug-and-play indoor trajectory monitoring system that layman users can easily set up by walking a one-minute loop trajectory after placing sensor nodes on walls. For practical scaling purposes, we consider using low cost COTS RF devices in distributed nodes. To be specific, we use COTS monostatic radars [25] in this study, each configured with a single pair of co-located transmitter and receiver. This radar facilitates interference-free simultaneous sensing by dithering phase for orthogonality [6] at the cost of cross-talk between nodes. Therefore, the distributed nodes can only measure the distance of the target based on the channel impulse response [6] but no pairwise distance measurement. While such configurations add to challenges from different levels, our design is without loss of generality because it works with minimum requirements on RF sensors and is applicable and compatible with more advanced RF devices (e.g., those with simultaneous communication and sensing) for self calibration. We will discuss further in Section 5.

Our Method. Taking into consideration the above challenges, we introduce a self calibrating algorithm that automatically estimates sensor locations using only distance measurements to the person walking in the monitoring space. The algorithm takes simultaneous observations from distributed nodes to optimize the estimation of relative sensor locations which minimize the distance measurement errors as an inverse process of multilateration, and we ensure its convergence at a unique solution by formulating it in a bipartite graph and analyzing its rigidity. Figure 1 shows the intuition of *SCALING* (**S**elf-**Cal**ibrating **In**door Tracking). This self calibrating process only takes a trivial effort without taxing layman users physically or cognitively, and the average computing time is within one minute and can concurrently finish at the stop of one-minute walking trajectory in the online mode. We evaluate our design via simulations and two real-world testbeds, one with dense deployment in a lab of 3×6 sq m and the other one with sparse deployment in a home configuration of sizes 4.5×8.5 sq m. Volunteers with no expertise in calibrating sensor placements were invited for data collection, during which they walked freely in the monitoring space without specific instructions to be followed and even without knowing where the sensors were mounted. According to volunteers' feedback, they all appreciated the easiness of the data collection process because they were not required to be trained or instructed to conduct walking freely, which only costed them about one minute on average. Experimental results demonstrate that our design achieves satisfying accuracy with the 80-percentile error of 53 cm in estimating the sensor locations and 40.5 cm in tracking the subjects, and largely outperforms a baseline with the adapted MDS, by 3.5 m/1.6 m in in 80-percentile error of self calibration and tracking, respectively. Notably, when comparing the tracking accuracy of self calibrated setup using our method against the classical multilateration with known sensor placements, we found that we can save hours of intensive calibrating effort with respective expertise to achieve comparable indoor tracking performance at the cost of only 1% degradation in accuracy, which is negligible.

Overall Contributions. We summarize our key contributions as follows:

- We propose *SCALING*, a plug-and-play device-free indoor trajectory monitoring system that a layman user can easily set up by walking a one-minute loop. It uses a self calibrating algorithm to eliminate the intensive manual efforts and technical expertise feasible with only researchers on calibrating the sensor placements (anchors) in prior work, paving the way for large scale self installation to benefit populations beyond small numbers of homes.
- We analyze self calibration of distributed sensor placements using only distance measurements in a bipartite graph, and ensure the uniqueness of its geometrical topology according to the graph rigidity. To achieve the convergence of self calibrating process, we introduce an iterative optimization in the mass-spring model [8] using a sequence of walking trajectory to address the uncertainty in self calibrating sensor placements for indoor localization/tracking.
- We implement a prototype of *SCALING* using low cost COTS monostatic UWB radars and evaluate our design in two real-world testbeds, one with dense deployment in a lab of 3×6 sq m and the other one with sparse deployment in a home configuration of 4.5×8.5 sq m, in addition to extensive simulations. Experimental results demonstrate that *SCALING* achieves satisfying accuracy with the 80-percentile error of 53 cm in estimating the sensor locations and 40.5 cm in tracking the subjects, accurate enough to extract informative daily in-home trajectories. When comparing the tracking accuracy of self calibrated setup using our method against the classical multilateration with known sensor placements, the results imply that we can save hours of intensive calibrating effort with respective expertise at the cost of negligible degradation in accuracy by 1%.

The remainder of this paper is organized as follows: Section 2 discusses the related work. Section 3 introduces *SCALING* with a self calibrating algorithm. Section 4 describes the evaluation of our design against the baseline. Finally, we discuss the limitations and opportunities in Section 5 and conclude in Section 6.

2 RELATED WORK

In this section, we discuss the relevant work in three categories: device-free monitoring, RF-based indoor tracking systems, and self calibration methods.

2.1 Device-free Monitoring

The device-free schemes for indoor monitoring are popular because of their user-friendly nature because they do not require users to carry any device to be monitored [38, 39]. In recent work, the concept of "structures as sensors" [42] becomes popular, which aims to indirectly sense humans and surrounding environments through their structural responses by using geophones or vibration sensors. However, such systems usually require costly refurbishment for large coverage [28, 30]. On the other hand, traditional methods using cameras with advanced computer vision methods [18, 40] are still useful for surveillance in the public space. Research also investigated acoustic sensors for in-home monitoring with prevalent IoT devices, e.g., Amazon Echo and Google Home [22, 35]. However, either vision based surveillance [18] or acoustic based monitoring [16] solutions are highly susceptible to background

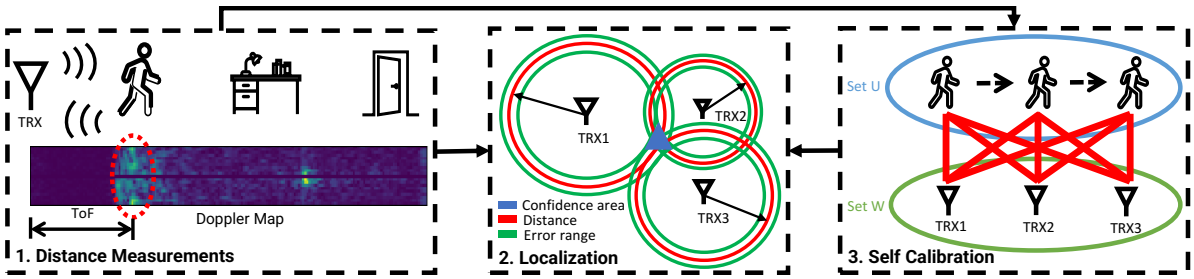

Figure 2: The overall framework of *SCALING* (Self-Calibrating Indoor Tracking), which has three major components: 1. Distance Measurements; 2. Localization; 3. Self Calibration. First, the human subject is detected for distance measurements in cluttered environment through the Doppler Map. Second, the simultaneous distance measurements from distributed nodes are fed to the multilateration algorithm for localization, given known sensor locations. Finally, a novel self calibrating algorithm formulates the problem in a bipartite graph and leverages its rigidity to obtain the uniqueness of geometrical topology for tracking trajectories of a walking person in the self calibrated local coordinate. With the first two components, we can build a device-free tracking system at cost of intensive manual effort and respective expertise on calibrating sensor placements. The third component estimates the relative sensor locations automatically, thus eliminating the need for manual calibration.

interference (lighting conditions or background noises) and sometimes may incur privacy concerns. We choose to exploit RF-based techniques, which is free of the aforementioned issues.

2.2 RF-based Indoor Tracking Systems

Because of preferable features of RF-based solution, people have widely explored localization/tracking using different RF techniques. WiFi devices [24, 37] are popular for research investigation in this field because of its ubiquitous feature. With recent rapid advancements, more COTS RF devices become available, and people start to look into FMCW [2, 3] and UWB [13, 41] for indoor sensing because of their fine-grained ranging resolution. For indoor tracking specifically, researchers developed various solutions based on different information, including proximity [9], fingerprinting [7], parameter joint estimation [32, 37], and triangulation (including trilateration and angulation) [24]. While such solutions were reported with promising results, they usually rely on well-calibrated sensor placements, which require hours of intensive manual setup and respective expertise, feasible only at small scale and by mostly researchers themselves. Scaling the deployments to tens or hundreds of real homes, however, would incur prohibitive manual efforts, and become infeasible for layman users. Some may argue that RF sensing systems with single-site configurations [1–4], can wrapped up in a compact box thus easy for scaling. However, their localization performance will degrade significantly when the subject is far away from the single-site sensors due to the fixed angle resolution [24], and when extending to multi-site setup to address this issue, coordinating their hand-off from one site to another still remains an open challenge [2]. Therefore, we build our system using distributed setups, which by nature eliminate the aforementioned issues by consistent coverage thus localization performance no matter where the subject is located.

2.3 Self Calibration

Self calibration [11, 27] is always a hot topic in the field of sensor networks, because it is a key enabler and promising for large scale deployment. We have seen a good body of work in self calibration for indoor localization/tracking. Research exploited prior knowledge about the participatory walking trajectory for self calibration [26] When the cross communication between neighbour nodes is available, Multidimensional Scaling (MDS) [14] has been applied for self calibration [10] given node-to-node distance measurements. Recent work leveraged MIMO platforms for self calibration, which is based on their satisfying space resolution to ensure the uniqueness of the pedestrian trajectory [23, 33]. However, the existing work either leverages the prior knowledge about the moving trajectories, or based on advanced RF platform with additional information than pure distance measurements. To the best of our knowledge, we are first to investigate self calibration using monostatic radars of minimum requirements (with only distance measurements to the walking subjects available).

3 SYSTEM DESIGN

In this section, we introduce *SCALING* (**S**elf-**Cal**ibrating **In**door Tracking), a plug-and-play device-free indoor trajectory monitoring system that a layman user can easily set up by walking a 1-minute loop, thus free of the intensive manual efforts and respective expertise. Our system uses distributed monostatic radars to collect concurrent distance measurements for localization. The key enabler of our system is a novel self calibrating algorithm that estimates sensor locations based purely on distance measurements to the person walking a sequence of unspecified trajectories in the monitoring space. Upon the convergence of self calibrating process, we use the estimated sensor locations as pseudo anchors for multilateration, different from the existing work using know sensor locations.

Figure 2 shows the overall framework of *SCALING*, which has three major components:

(1) Distance Measurement (Section 3.2): Each distributed monostatic radar measures the distance of the subject away from it according to ToF of the emitted signal bounced off the human body back to the corresponding receiver.
(2) Localization (Section 3.3): We can apply multilateration to localize the subject when the distance measurements of a subject in the monitoring area are available from distributed nodes, assuming the locations of distributed nodes are known.
(3) Self Calibration (Section 3.4): When the locations of distributed nodes are unknown and the only available information is the distance measurements to the human subject walking unspecified trajectories in the monitoring area, we form the problem in a bipartite graph, of which the edges are the distance measurements between the unknown sensor locations and unknown participatory step locations in walking trajectories. With only distance measurements as constraint, the vertices may flex thus varying the geometrical topology of the bipartite graph. With the analysis of graph rigidity to ensure the uniqueness of the geometrical topology, we use iterative optimization to reach convergence of estimated sensor locations.

Before getting into the technical details, we first discuss the design considerations in (Section 3.1) to help shape the problem.

3.1 Design Considerations

Out of practical considerations for future large scale deployment of device-free indoor tracking systems, we have to balance trade-offs among several key factors: localization/tracking performance, deployment efforts on well-calibrated sensor placements, and cost of RF sensor nodes. Distributed configurations provide consistent localization/tracking performance in contrast to single-site configurations, at the price of prohibitive deployment cost. Therefore, we are challenged to minimize the deployment cost, which mainly comes from intensive efforts in calibrating sensor placements with careful measurements and respective expertise, in addition to the expense of sensor nodes.

Hardware Choices. While we know the goal of hardware choices is to minimize the expense of sensor nodes, it is non-trivial to understand what it takes to meet the minimum requirements for device-free indoor tracking:

- For the minimum overhead on communication, we consider the case that sensor node will only forward measurement data to the central server for computations, but there is no cross-talk among sensor nodes to exchange information.
- Each node has to be configured with at least one transceiver so that multilateration can be applied for localization with distance measurements from distributed nodes.
- The critical but tricky part is that we have to ensure the orthogonality of RF signals for simultaneous sensing with distributed nodes, when the coordinated transmission is unavailable with no cross-talk.

To address the above concerns all together, we use a low cost COTS UWB sensor [25] which achieves orthogonality by dithering phase [6], such that concurrently emitted signal will not interfere each other even in the absence of cross-talk to coordinate transmission among distributed nodes. This COTS UWB sensor is a monostatic radar, configured with a single pair of co-located transmitter and receiver. It measures the distance of the target according to the time of flight (ToF) of the repeatedly emitted signal bounced off from the target and captured by the receiver. Herein, we clarify our hardware choices to meet minimum requirements for device-free indoor tracking.

Design Goals. The remaining issue to minimizing the deployment cost is to mitigate the intensive efforts in calibrating sensor placements with careful measurements and respective expertise. That unveils the major goal of this paper, which is to design a plug-and-play device-free indoor tracking system using low cost COTS RF devices. And the key enabler of this system is a novel self calibrating algorithm, that eliminates the need for intensive manual calibrating effort on sensor deployment. While this design goal is derived from the configuration of minimum requirements premised on specific hardware choices, we believe the discussion of such design is without loss of generality, because it works with RF sensors of minimum requirements and is applicable and compatible with more advanced RF devices for self calibration [23, 33]. We will discuss how our design can be applied to advanced RF devices given more features in Section 5.

3.2 Distance Measurement

As clarified in Section 3.1, we use low cost COTS UWB radars at the band 7.25-10.2 GHz in distributed nodes for distance measurements, and this UWB radar was designed with swept-threshold sampling with cumulative 1-bit quantized value [6], enabling a high-speed sampler that operates at 23.328 GS/s, sufficient to sample received signals at high resolution. With that, it may appear to be straightforward to obtain distance measurements to the human subject as the time of flight (ToF) can be estimated according to the delay between transmission of short UWB pulses and receiving the signals reflected by the human body. However, two key factors challenge reliable distance measurements: 1) The multi-path effect may cause ambiguity in differentiating the human subject from the static objects in the cluttered environment. 2) The human body is more complex than a point scatterer, so echoes may come from the head, arms, legs, and torso, which span dozens of centimeters in space, introducing ambiguity in determining the actual distance between the human subject and sensor nodes.

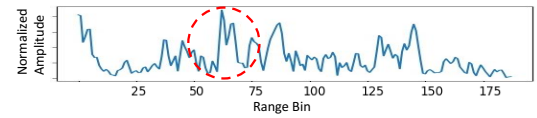

(a) Range profile from CIR.

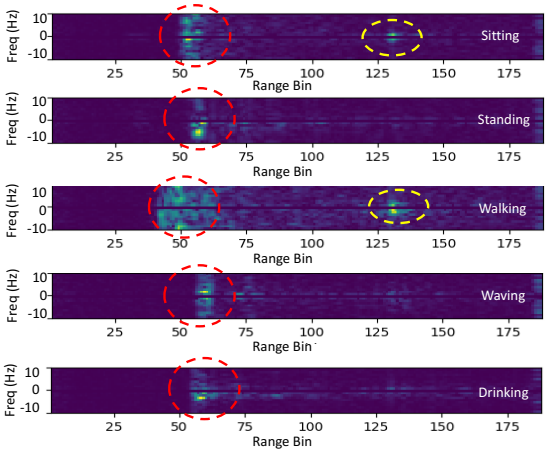

(b) Doppler maps of different activities.

Figure 3: Figure (a) shows a range profile, where the channel impulse response due the human subject is not easily distinguishable. Figure (b) shows Doppler maps of different activities. The x-axis of the Doppler map is the index of range bins, corresponding to the distances aligned with the range profile; y-axis shows the index of frequency band determined by the length of time window and the frame rate of the range profiles. The color code of the plot corresponds to a heat-map of the intensity in the reflected signal. Strong reflectors are indicated by light colors such as yellow and green, weaker reflectors are indicated by dark blue, and the absence of a reflector is indicated by black at the corresponding frequency. The red circles indicate the reflection from a human subject, and the yellow circles indicate the multi-path components.

To localize human subjects, we first have to detect them from the cluttered environment, so we need to eliminate the impact from static reflectors. Figure 3(a) shows the range profile generated directly sampled Channel Impulse Response (CIR), from which the reflection from human body is not prominent for detection. The x-axis of the range profile is the index of range bins, linearly proportional to the distance; y-axis shows the normalized amplitude of the received signal; a point in the curve of the range profile indicate the intensity of the reflection from a certain distance. We detect the human subject by leveraging the observation that signals from static reflectors are constant in both amplitude and phase over time, different from Doppler effects caused by moving subjects.

We visualize the Doppler effects [21] in the reflected signal with Doppler maps [12] by applying Short-Time Fourier Transform to a

sequence of consecutive range profiles along the time dimension. Figure 3(b) shows five Doppler map examples, of which the data was collected when performing five typical indoor activities. While the patterns of Doppler maps may differ between different activities, the moving human subject is always highlighted with prominent intensity in the Doppler map.

After eliminating static components, we notice that the signals reflected from human body may spread thin in a wide chunk because different body parts move differently and the corresponding reflections may interfere each other constructively or destructively. Besides, the Doppler map may show the highest intensity at a distance other than where the human subject is located due to dynamic multi-path components [3], which are the reflections that bounce off the human body then bounce off static objects in the cluttered environment before arriving at the receiver. To reduce the ambiguity from the dynamic multi-path components, we reject them based on that fact that dynamic multi-path signals are always traveling longer paths and coming later than the direct reflections from the human body. To be specific, we apply CFAR [36] to detect pixels in the Doppler map corresponding to the valid reflections and take the closest chunk of detected pixels as the reflections from human body according, and the distance measurement to the human subject is calculated as the distance to the mass centroid of the closest chunk:

$$d_{mc} = \lim_{\Delta m \to 0} \frac{\sum_{i=1}^{N} \sum_{j=1}^{M} \Delta m_{ij} d_j}{\sum_{i=1}^{N} \sum_{j=1}^{M} \Delta m_{ij}}, \quad (1)$$

where i is the index of total N frequency bands, j is the index of total M range bins, Δm_{ij} is the intensity of the pixel at the index of (i, j) in the Doppler map, and d_j is the corresponding distance of the range bin of index j.

3.3 Localization

As discussed in Section 3.1, we aim to develop a device-free tracking system using low cost RF sensors of minimum requirements thus without loss of generality. Therefore, the only available information for localization is the distance measurements through the time of flight, but the angle of arrival is not available due to the limited space diversity of the monostatic radar configured with a single pair of co-located transmitter with receiver. To achieve angle information with limited space diversity, some existing work [4] explored a classical radar technique called inverse synthetic aperture radar (ISAR) [29], which emulates a virtual antenna array in the reference system of the moving target. While this method was able to detect sharp changes in the angle, it is not applicable for fine-grained trajectory tracking, because the angle resolution of ISAR methods, determined by the time window of observations, is relatively low and not sufficient to capture the walking movement of low speed and changing direction. The coarse-grained angle information from ISAR may add some constraints for localization through joint parameter estimation, it is out of the scope of this paper. We will focus on the discussion of using distance measurements only for localization.

After detecting the human subject in the cluttered environment by addressing ambiguities from multi-path effects with the Doppler map, each sensor node obtain reliable distance measurements to the human subject. Then, we can combine simultaneous distance measurements from distributed nodes for localization. Given known sensor locations, we can easily estimate the location of the human subject which gives the least squared error of distance according to their respective distance measurements. For simplicity, we illustrate localization in 2D plane as shown in the middle part of Figure 2. When we consider just one transceiver, one distance measurement can form one circle around the sensor location, indicating the confidence area where the human subject is located assuming no other constraints applied. At any time, if there are at least three distributed sensor nodes available for simultaneous distance measurements, we can find a intersection between three circles to locate the human subject. To generalize the argument to localization in 3D space, we only need one additional sensor node. While three distributed sensor nodes are sufficient for getting a unique estimate of the human subject's location in 2D plane, we notice that increasing the number of sensor nodes can help reduce the uncertainty in localization with noisy distance measurements. Figure 4 shows the uncertainty of localization can be reduced with increasing number of sensor nodes. We will study the impact of the number of sensor nodes on our design in Section 4.

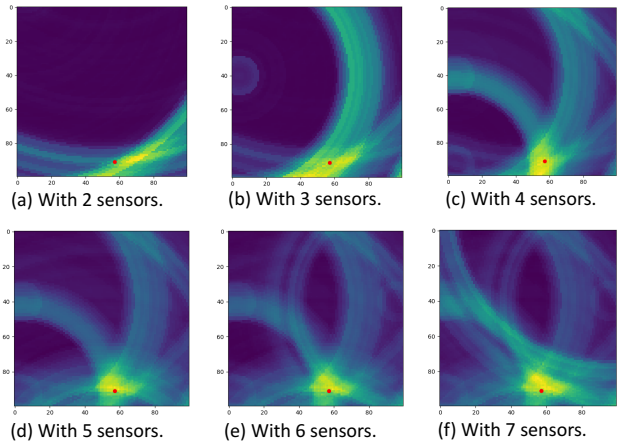

Figure 4: We use different number of sensors to localize a target in a 1m×1m space. The red dot indicates the ground truth of the human subject's location. With increasing number of sensor nodes, the intersection region is with less uncertainty, thus more accurate,

3.4 Self Calibration

With the previous two design components, we can build a reliable device-free indoor localization/tracking system if we could afford the intensive effort for calibrating the sensor placements. However, it becomes prohibitively expensive when scaling such system to large scale deployment. To address that, this section introduces a novel self calibrating algorithm that estimates the relative sensor locations through purely the distance measurements to walking trajectories of the human subject in the monitoring area by leveraging the rigidity of bipartite graph. This estimated sensor locations are used as anchors for localization/tracking together with the previous two design components. The proposed self calibrating algorithm largely reduces hours of intensive calibrating efforts with respective expertise to merely one-minute walking affordable by layman users at cost of negligible loss in localization/tracking accuracy.

We first describe our self calibrating algorithm that estimates the relative sensor locations using merely distance measurements to the walking trajectories. We also describe a relevant method and discuss why it is not applicable in this problem, and how we adapt it as a supplementary process.

3.4.1 Self Calibrating Algorithm. Consider M sensor nodes distributed at unknown locations in the monitoring space. As described in Section 3.1, we assume each node can only measure the distance to the present human subject, but not node-to-node pairwise distance because their signals are orthogonal thus no cross-talk.

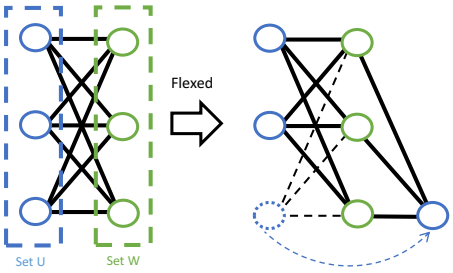

Figure 5: In this example graph, a vertex in Set U could flex while preserving the distances.

Distance measurements are available for N step locations in the walking trajectories of the human subject. The task is formed as to estimate the relative sensor locations using distance measurements only. For clarity, we assume the following discussion of localization/tracking is in 2D plane ($\mathbb{R}^2$) if not specified; the 3D version is a simple and natural extension.

We first analyze whether it is a solvable problem and in what conditions. When the problem is modeled in a linear system, a natural but naive way is to check whether it has more independent equations of constraints/observations than the number of unknowns. However, our problem is modeled with constraints from distance measurements, which is quadratic but not linear, so the necessary and sufficient conditions for solvability of linear systems are not applicable here. We formulate the problem in a graph $G(V, E)$, as illustrated in the third part of Figure 2, to determine whether it is solvable to estimate relative sensor locations by analyzing the uniqueness of the geometrical topology. V denotes the vertices, including M sensor locations (denoted as $a_i \in W$) and N step locations (denoted as $p_j \in U$) in walking trajectories where the distance measurements to the human subject are taken. E denotes the edges, corresponding to the distance measurements d_ij between the sensor locations a_i and step locations p_j. Apparently, this graph is a bipartite graph and is a complete bipartite graph because there is no edge among the subsets of sensor locations W or step locations U, every edge in $G(V, E)$ connects a vertex in W to one in U, and every pair of vertices between Set W and Set U are connected.

We note that the coordinate assignments thus the geometrical topology of the bipartite graph may not be unique even up to rotation, translation, and reflection, because certain vertices could flex while preserving the distances, as illustrated in Figure 5. To obtain a unique geometrical topology, the graph has to be globally rigid [19, 20]. According to characteristics of the globally rigid graph [17, 31], several conditions need to be met:

(1) The distribution of vertices (including sensor locations and step locations) needs to be generic, thus no three vertices form a line like the distribution of Set W in Figure 5.
(2) Applying Euler's formula gives the relation between the number of edges l and the number of vertices m, $l \geq 2m - 3$. In our case, $l = M \times N$, $m = M + N$, so we get $M \geq 2 + \frac{1}{N-2}$ and $N \geq 2 + \frac{1}{M-2}$.
(3) Globally rigid graph needs vertices to be (d+1)-connected in $\mathbb{R}^d$, thus 3-connected in 2D, met by nature of the complete bipartite graph.

The last two conditions can be easily met when we use least three sensor nodes and three step locations. For the first condition, we can distribute sensor nodes to different walls around the monitoring space to avoid forming a line. Although step locations in walking trajectories may fail to meet the first condition due to randomness, however, people usually would not walk along a perfectly straight line in natural settings. By randomly selecting step locations from a walking trajectory, it is a rare case that three step locations form a line, and can be mitigated with iterative optimization.

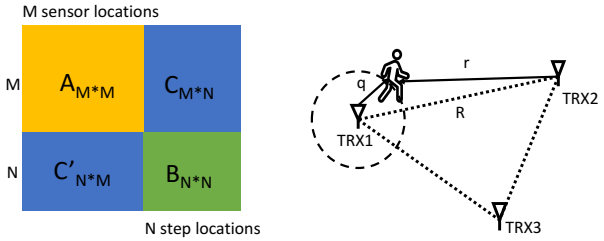

(a) Distance matrix. The sub-matrix A/B denotes the pairwise distance measurements within sensor/step locations (Set W/U). Sub-matrices C and C' denote distance measurements across sensor locations Set W and step locations Set U.

(b) The step location close to a certain sensor location opens the opportunity to approximate the sensor-to-sensor distance measurements with sensor-to-step distance measurements for MDS to achieve initial topology.

Figure 6: While distance measurements are only available in C and C', we can use sensor-to-step distance measurements to approximate sensor-to-sensor distance measurements. Therefore, we can use MDS to achieve an initial coordinate assignment with an approximate sensor-to-sensor distance matrix A'.

Now we are confident about the solvability of our problem, and can focus on estimating the sensor locations through distance measurements to the step locations in walking trajectories. With the graph, our goal is to generate a geometrical topology in which the coordinate assignments of sensor locations $a_i \in W$ and step locations $p_j \in U$ are consistent with all distance measurements d_{ij}, $\|a_i - p_j\| = d_{ij}$ for all $d_{ij} \in G(V, E)$. Therefore, we can estimate of sensor locations by optimizing each residual between the measured distance d_{ij} and the estimated distance (between the estimated sensor location a_i and the corresponding step location p_j), defined as $e = |\|a_i - p_j\| - d_{ij}|$. We adapt it in the mass-spring model for optimization, where each edge in the graph is taken as a spring between two masses, with a rest length equal to the measured distance. When the estimated distance between a_i and p_j is shorter than the measured distance, the spring incurs a force that pushes two nodes apart. Similarly, when the estimated distance is larger than the measured distance, the spring pulls them together. Along the optimization process, the estimated nodes move in the direction of the resulting force of the spring. The stress of this mass spring model to be optimized is expressed as:

$$\text{Stress} = \frac{\sum \left(d_{ij} - \|a_i - p_j\|\right)^2}{\sum \|a_i - p_j\|^2} \tag{2}$$

When the stress becomes zero, the whole mass-spring system reaches equilibrium, so the optimization process reaches the global minimum. We empirically choose Sequential Least Squares Programming (SLSQP) as the optimization solver. Because the measured distance is noisy, the estimated sensor locations are expected to jiggle to a certain extent. Instead of using one-time estimated sensor locations W, we combine results from multiple rounds. At the k-th round, we select a set of step locations along walking trajectories (denoted as U_k) with corresponding distance measurements to estimate the configuration of sensor locations (denoted as W_k). A new round of self calibrating process will be executed with a new set of step locations U_{k+1} until the residual difference between W_k and W_{k-1} reaches a small empirical threshold.

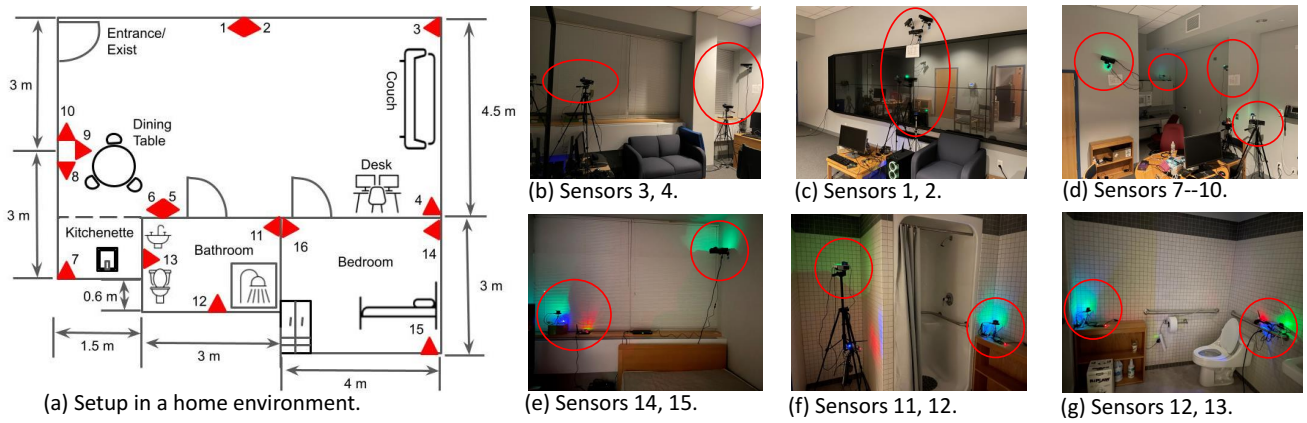

(a) Setup in a home environment. (b) Sensors 3, 4. (c) Sensors 1, 2. (d) Sensors 7--10. (e) Sensors 14, 15. (f) Sensors 11, 12. (g) Sensors 12, 13.

Figure 7: The testbed with sparse deployment in a cluttered home environment decorated with furniture.

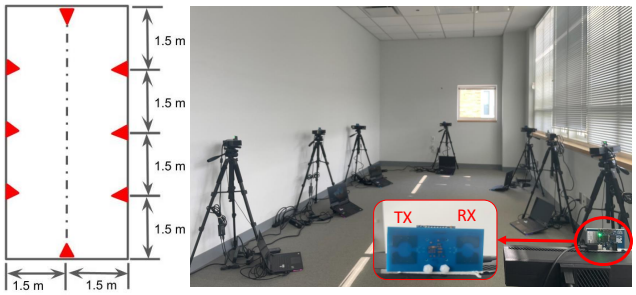

(a) Setup in a small lab. (b) Testbed with dense deployment.

Figure 8: The testbed with dense deployment in a lab environment.

3.4.2 Approximate MDS for Initial Coordinate Assignment. While the mass-spring model is powerful for self calibrating process, it has a chance to converge at local minimum if it starts with a random initial coordinate assignment. We aim to introduce a supplementary process that provides the self calibrating process with a reliable initial coordinate assignment with a similar geometrical topology to the ground truth, such that the mass-spring model can easily converge at a global minimum rather than a local minimum. One relevant method, Multidimensional Scaling (MDS) [14], is often used as a dimension reduction technique to graphically visualize data in 2D, and can be applied to convert distance measurements between nodes into node locations [43]. While MDS requires a complete set of node-to-node distance measurements, it is not available in our problem as illustrated in Figure 6(a): we only have available distance measurements across sensor locations Set W and step locations Set U in sub-matrices C and C', but the pairwise distance measurements within Set W or Set U corresponding to sub-matrices A or B are not available. The fact that certain step locations in random trajectories are close to a certain sensor location opens the opportunity for using MDS with approximate node-to-node distance measurements for initialization. As shown in Figure 6(b), given a step location close to a certain sensor node 1, we obtain the triangle inequalities: $r - q < R < r + q$. According to the Squeeze Theorem, we can use the sensor-to-step distance r to approximate the sensor-to-sensor distance R when q is relatively small. Notably, because MDS requires the distance matrix to be positive semi-definite, we keep the elements symmetric to the diagonal by using the one closer to the sensor among a pair. Therefore, we can use MDS with the approximate sensor-to-sensor distance matrix A' for initialization of coordinate assignments.

4 EVALUATION

To evaluate our design, we conducted extensive experiments via two real-world testbeds as well as simulations. We first describe the experimental setups, the purpose experiments we conducted and the metrics and ground truth used for evaluation in Section 4.1. Then, the experimental results with real-world testbeds are presented in Section 4.2. We also conduct extensive simulations to study the impact of different factors on the end-to-end performance in Section 4.3.

4.1 Experimental Methodologies

To collect real-world data for evaluation, we built two testbeds, one with sparse deployment in a cluttered home environment of size 4.5×8.5 sq m, shown in Figure 7, and the other one with dense deployment in an empty lab environment of 3×6 sq m, shown in Figure 8. Notably, settings in two testbeds configured with redundant sensors on tripods are for research purpose only. A much smaller number of sensors (e.g., mounted on walls) would be sufficient in real-world scenarios. The UWB signal can sense human movements through the wall/door with penetration ability [1], thus can be shared across different rooms to further reduce the number of necessary sensor nodes. In each sensor node, we use a COTS IR-UWB sensor XeThru x4m03 [25] as a monostatic radar for distance measurements. The emitted pulse is configured with the frequency band 7.25-10.2 GHz centered at 8.75 GHz, and the sampling frequency of this COTS UWB sensor is 23.328 GHz, sufficient to capture reflections with a high resolution. The frame rate of the UWB sensor is configured to be 20 frame-per-second (fps), thus able to update distance measurements 20 times per second, and its measurement range is up to 10 meters. Distributed sensor nodes are synchronized through the Network Time Protocol (NTP), and concurrent sensing data (e.g., distance measurements) are forwarded to an on-site central server in batches and aligned according to the associated timestamps at a resolution of 0.05 sec for further computation (e.g., self calibration and localization/tracking) in a retrospective manner.

4.1.1 Data Collection and Experiments. For data collection, we invited volunteers with no expertise in calibrating sensor placements, and they walked freely in the monitoring space without specific instructions and without knowing the sensor locations to generate random walking trajectories thus emulating the natural indoor trajectories as users will be performing in a real world scenario. According to the feedback from volunteers, they were not feeling challenged physically or cognitively during data collection, because

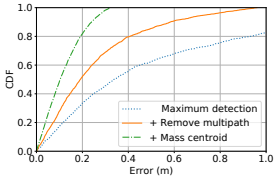

Figure 9: Comparison of distance measurements between methods with challenging issues addressed progressively.

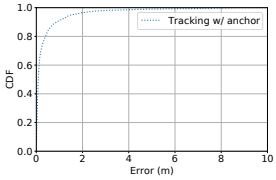

Figure 10: Tracking performance using distance measurements with known sensor locations.

it was as simple as taking a walk in a room for about one minute, even though they did not take any training program to prepare them for that. During data collection, we follow a pre-established protocol that protected the anonymity of the students. We use 50% of collected data for evaluation of self calibrating algorithm and the remaining 50% for evaluation of end-to-end tracking performance using the self calibrated sensor locations. We also use the approximate MDS described in Section 3.4.2 as a baseline for comparison and compare the end-to-end performance with and without the approximate MDS for initial coordinate assignments. In addition, we conducted extensive simulations to study the impact of different factors, including the accuracy of distance measurements, the number of sensor nodes, the number of step locations, and the number of optimization rounds.

4.1.2 Metrics and Ground Truth. To better understand the performance of our system, we evaluate the performance of three design components (i.e., distance measurement, localization and self calibration) and their impacts on the end-to-end performance, respectively. We use the distance error (i.e., the residual error between the ground truth distance and measured distance, $e_d = |d - \hat{d}|$) to evaluate the distance measurement module, and use the localization error (i.e., the residual error between the ground truth position and estimated position, $e_p = \|p - \hat{p}\|$) to evaluate the localization and self calibration modules. For easy evaluation, we transformed the estimated relative sensor locations from the self calibrating process in a local coordinate system to align with the global coordinate system through Procrustes analysis [15] (with a composition of translation, rotation, and reflection).

We use Kinect XBox which incorporates a human body pose recognition model [34] to detect human bodies with its embedded depth sensor. The depth sensor by nature can provide measure of the distance and position of detected persons relative to the depth sensor, and they are recorded as ground truth. For simplicity, we mount each UWB sensor on top of a Kinect depth sensor, so that they are co-located for comparison. In addition to the ground truth from the depth sensor, we also use some fixed pre-known locations and trajectories as the ground truth for evaluation.

4.2 Experiments with Real-world Testbeds

We first evaluate the performance of distance measurements with UWB monostatic radars to characterize the distance error at a single sensor node. Then, we evaluate the localization module using simultaneous distance measurements from distributed sensor nodes assuming the sensor locations are known. Finally, we evaluate the self calibrating algorithm compared to using MDS only as well as combining with MDS for initialization.

4.2.1 Distance Measurement. Figure 9 shows CDF of distance measurement error compared to naive methods which do not address issues due to the multi-path effects and/or spread scatterer of human body. The results indicate an incremental improvement in the

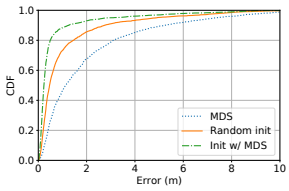

(a) Comparison of self calibration in CDF.

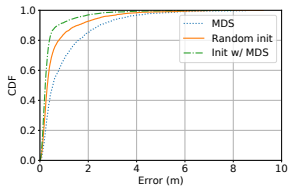

(b) Comparison of tracking after self calibration in CDF.

Figure 11: Our proposed method with random initial coordinate assignments outperforms the adapted MDS as a baseline. With MDS for initial coordinate assignment, the performance is further improved.

distance measurements by addressing challenges from the static reflection and dynamic multi-path components in the cluttered environment progressively. With all issues addressed using our method, we achieve the median error of distance measurements about 10 cm.

4.2.2 Localization. Figure 10 shows the error distribution of localization using known sensor locations, and our system can achieve a 80-percentile error of 40.1 cm, which is promising for indoor trajectory tracking and corresponding analytics. However, using known sensor locations means such performance is achieved at the cost of hours of intensive manual calibration of sensor placements, which hinders large scale deployment of such systems.

4.2.3 Self Calibration. Figure 11(a) shows the error distribution of self calibrated sensor locations. Figure 11(b) shows the error distribution of tracking performance using the estimated sensor locations after self calibration. We observe that the performance of using MDS alone is not satisfying and of large variability due to its dependency on the step locations which is of large randomness. On the other hand, using MDS for initial coordinate assignment does improve the performance of self calibration, thus end-to-end tracking performance with a 80-percentile error of 40.5 cm. The proposed self calibrating method combined with the adapted MDS for initial coordinate assignments outperforms the adapted MDS as a baseline by 3.5m/1.6m in in 80-percentile error of self calibration and tracking, respectively. Observations that tracking errors are smaller than self calibration errors can be explained by that complementary information in multilateration with redundancy mitigates the impact from the error in estimated sensor locations. It is also interesting to observe that the tracking performance with noisy estimated sensor locations is comparable to the tracking performance with known sensor locations. Such an observation implies that our system can save hours of intensive manual calibration efforts at the cost of negligible degradation in tracking performance by mere 1%.

4.3 Factor Study with Simulations

To better understand the effectiveness of our design, we conducted extensive simulations to examine the impact of different factors on the system, including the accuracy of distance measurements, the number of sensor nodes, the number of step locations, and the number of optimization rounds. To evaluate *SCALING* with simulations, we randomly generate coordinates of distributed sensors and steps, as well as noisy distance measurements between them. The default setting is configured with 5 sensor nodes, 9 step locations, 1 optimization rounds, and the Gaussian noise of 10 cm in distance measurements. When we vary one factor, the other parameters remain unchanged if not specified in the following discussion. We believe such knowledge can help form some guidelines to improve the performance and lead to more effective sensor deployment.

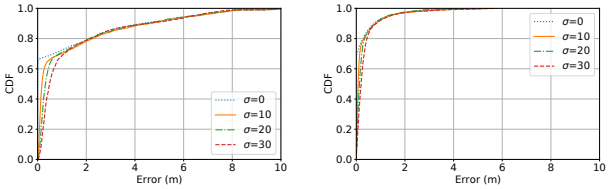

(a) Self calibration performance with varying accuracy of distance measurements.

(b) Tracking performance with varying accuracy of distance measurements.

Figure 12: With better accuracy of distance measurements, a better performance can be achieved in both self calibration and tracking.

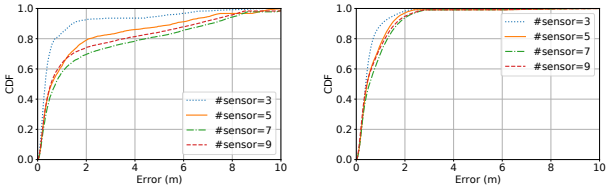

(a) Self calibration performance with varying number of distributed sensor nodes.

(b) Tracking performance with varying number of distributed sensor nodes.

Figure 13: With increasing number of distributed sensor nodes, it is harder to achieve convergence of self calibration, thus worse estimate of sensor locations. However, the tracking performance is comparable among different number of sensor nodes, because the tracking error was mitigated by the redundancy of the anchors where a portion of them are well calibrated.

4.3.1 Accuracy of Distance Measurement. To understand how the accuracy of distance measurements will impact system, we simulate distance measurements with Gaussian noise of different standard deviations, varying from 0 to 30 cm. Figure 12(a) shows the performance of self calibration with different accuracy levels. Figure 12(b) shows the tracking performance with different accuracy levels after self calibration. Both results indicate that the accuracy of distance measurements is vital to both self calibration and tracking.

4.3.2 Number of Distributed Sensor Nodes. In previous discussion, we conjectured that increasing the number of sensor nodes can reduce in the uncertainty in localization with multilateration. To examine the conjecture, we vary the number of distributed sensor nodes from 3 to 9. Figure 13(a) shows the performance of self calibration with increasing number of sensor nodes. Surprisingly, the self calibration error becomes larger with more sensor nodes. That can be explained by the fact that more sensor nodes add uncertainty in the geometrical topology, and a small portion of nodes may flex while preserving constraints in distance measurements. Figure 13(b) shows the tracking performance with increasing number of sensor nodes. Counter-intuitively, the tracking performance remains similar with increasing number of sensor nodes, even though their calibration performance degrades. It can be explained by the fact that multiple (redundant) anchors can compensate the noisy location of each other owe to the merit of multilateration based tracking method. This observation implies that a small number of nodes would provide sufficient accuracy, while partitioning may need to be considered for self calibration to cover a large space.

4.3.3 Number of Step Locations. We compare the self calibration performance with different number of step locations and the resulting tracking performance with self calibrated sensor locations. Figure 14(a) shows the performance of self calibration with different number of step locations. Figure 14(b) shows the tracking performance based on sensor locations calibrated with different number of step locations. Interestingly, we observe a consistent trend in that increasing the number of step locations improve the performance of both self calibration and tracking. Such an observation suggest using more step locations will help improve the end-to-end performance.

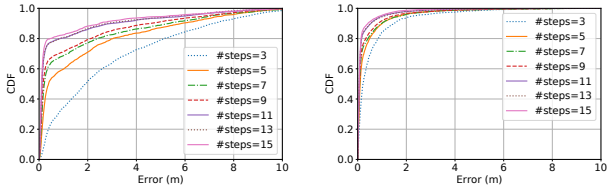

(a) Self calibration performance with varying number of step locations.

(b) Tracking performance with varying number of step locations.

Figure 14: With increasing number of step locations, both self calibration and tracking are getting better performance.

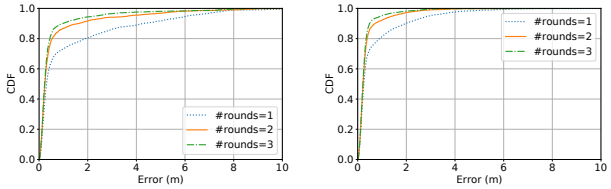

(a) Self calibration performance with varying number of optimization rounds.

(b) Tracking performance with varying number of optimization rounds.

Figure 15: With increasing number of optimization rounds, both self calibration and tracking are getting better performance.

4.3.4 Number of Optimization Rounds. The optimization process for self calibration may converge at a local minimum with distorted topology due to noisy distance measurements and random step locations. Multiple rounds of optimization can help mitigate convergence at the local minimum. We observe improvements in performance of both self calibration and tracking given more rounds for self calibration in Figure 15(a) and Figure 15(b), respectively.

5 DISCUSSION

In this section, we discuss the limitations and opportunities to guide future work.

Scalability. For clarification, the term "large scale deployment" in this paper specifically refers to scaling deployments to a good number (e.g., tens or hundreds) of homes of diverse layouts. Covering one site with large indoor spaces (e.g., a transportation hub) is a different issue: while self calibration with a small number (e.g., 3–5) of sensor nodes can be reasonably accurate, more nodes do not necessarily lead to better performance due to increasing uncertainty of sensor placements. In the future, we will explore dynamically partitioning a large area and optimizing the self calibration in each partition (e.g., with only three closest nodes). To adapt *SCALING* to co-habiting scenarios, we can follow the previous work to achieve multi-user tracking using successive interference cancellation [2].

Compatibility and extensibility with various RF devices. The choice of the COTS UWB used in this paper is a trade-off between several factors, including its range resolution for distance measurements, orthogonality for simultaneous sensing of distributed nodes, and low price. With this hardware choice, *SCALING* demonstrates its generazability with RF sensors of minimum requirements. It is noted that such a trade-off is achieved within the

scope of COTS RF devices. We can further optimize such a trade-off with our customized RF design. Ingoring practical concerns about the cost, *SCALING* is compatible with other COTS RF techniques, and can be easily extended when additional information becomes available. Three possible cases are: 1) a better accuracy can be achieved using RF techniques of finer range resolution, e.g., mmWave. 2) When using RF sensors configured with phased array antennas instead of a single transceiver, additional AoA measurements can be integrated to further reduce the ambiguity in self calibration and localization. 3) When the cross-communication between nodes is available, we can apply the classical MDS with a complete distance matrix instead of the approximate one for more reliable initial coordinate assignment.

Daily indoor trajectory analysis. We plan to scale data collection to tens or hundreds of real homes with easy self-installation enabled by *SCALING* so that we can focus more on health analytics with long-term daily indoor trajectories. We believe daily indoor trajectories would carry more information than just the occupancy state of inhabitants in a certain space. For example, daily trajectories can be used for profiling the ambulation ability of inhabitants, and changes in patterns such as decreasing activities in the kitchen might indicate declines in cognitive and physical abilities, early indicators for people at risks of diseases like Alzheimer's.

6 CONCLUSION

We propose *SCALING*, a plug-and-play device-free indoor trajectory monitoring system that a layman user can easily set up by one-minute walking. It uses a self calibrating algorithm to save hours of intensive manual efforts and technical expertise at the cost of negligible degradation in end-to-end performance. We believe *SCALING* opens door for large scale deployment of in-home monitoring system, manageable by relatively small size research teams, thus potentially benefiting large populations beyond a handful of homes.

REFERENCES

[1] Fadel Adib, Chen-Yu Hsu, Hongzi Mao, Dina Katabi, and Frédo Durand. 2015. Capturing the human figure through a wall. *TOG* 34, 6 (2015), 1–13.

[2] Fadel Adib, Zachary Kabelac, and Dina Katabi. 2014. Multi-person motion tracking via RF body reflections. (2014).

[3] Fadel Adib, Zach Kabelac, Dina Katabi, and Robert C Miller. 2014. 3D tracking via body radio reflections. In *NSDI 14*. 317–329.

[4] Fadel Adib and Dina Katabi. 2014. See through walls with WiFi!. In *SIGCOMM*.

[5] Fakhrul Alam, Nathaniel Faulkner, and Baden Parr. 2020. Device-free localization: A review of non-RF techniques for unobtrusive indoor positioning. *IEEE Internet of Things Journal* 8, 6 (2020), 4228–4249.

[6] Nikolaj Andersen, Kristian Granhaug, Jørgen Andreas Michaelsen, Sumit Bagga, Håkon A Hjortland, Mats Risopatron Knutsen, Tor Sverre Lande, and Dag T Wisland. 2017. A 118-mW pulse-based radar SoC in 55-nm CMOS for non-contact human vital signs detection. *IEEE Journal of Solid-State Circuits* (2017).

[7] Paramvir Bahl and Venkata N Padmanabhan. 2000. RADAR: An in-building RF-based user location and tracking system. In *IEEE INFOCOM (2000)*.

[8] Kenneth Batstone, Magnus Oskarsson, and Kalle Åström. 2016. Robust time-of-arrival self calibration and indoor localization using Wi-Fi round-trip time measurements. In *2016 IEEE ICC*. 26–31.

[9] Valentina Bianchi, Paolo Ciampolini, and Ilaria De Munari. 2018. RSSI-based indoor localization and identification for ZigBee wireless sensor networks in smart homes. *IEEE Transactions on Instrumentation and Measurement* (2018).

[10] Klemen Bregar, Andrej Hrovat, Mihael Mohorčič, and Tomaž Javornik. 2020. Self-Calibrated UWB based device-free indoor localization and activity detection approach. In *EuCNC 2020*. IEEE, 176–181.

[11] Vladimir Bychkovskiy, Seapahn Megerian, Deborah Estrin, and Miodrag Potkonjak. 2003. A collaborative approach to in-place sensor calibration. In *Information processing in sensor networks*. Springer, 301–316.

[12] Victor C Chen, Fayin Li, S-S Ho, and Harry Wechsler. 2003. Analysis of micro-Doppler signatures. *IEE Proceedings-Radar, Sonar and Navigation* 150, 4 (2003), 271–276.

[13] Yuechun Chu and Aura Ganz. 2005. A UWB-based 3D location system for indoor environments. In *2nd International Conference on Broadband Networks, 2005.* IEEE.

[14] Michael AA Cox and Trevor F Cox. 2008. Multidimensional scaling. In *Handbook of data visualization*. Springer, 315–347.

[15] Marco Crocco, Alessio Del Bue, and Vittorio Murino. 2011. A bilinear approach to the position self-calibration of multiple sensors. *IEEE Transactions on Signal Processing* 60, 2 (2011), 660–673.

[16] Nakul Garg, Yang Bai, and Nirupam Roy. 2021. Owlet: Enabling spatial information in ubiquitous acoustic devices. In *MobiSys 21*. 255–268.

[17] Steven J Gortler, Alexander D Healy, and Dylan P Thurston. 2010. Characterizing generic global rigidity. *American Journal of Mathematics* 132, 4 (2010), 897–939.

[18] Kai Guan, Lin Ma, Xuezhi Tan, and Shizeng Guo. 2016. Vision-based indoor localization approach based on SURF and landmark. In *IWCMC 2016*. 655–659.

[19] Bruce Hendrickson. 1992. Conditions for unique graph realizations. *SIAM journal on computing* 21, 1 (1992), 65–84.

[20] Gareth Jones, Roman Nedela, and Martin Škoviera. 2008. Complete bipartite graphs with a unique regular embedding. *Journal of Combinatorial Theory, Series B* 98, 2 (2008), 241–248.

[21] Youngwook Kim, Sungjae Ha, and Jihoon Kwon. 2014. Human detection using Doppler radar based on physical characteristics of targets. *IEEE Geoscience and Remote Sensing Letters* 12, 2 (2014), 289–293.

[22] Dong Li, Jialin Liu, Sunghoon Ivan Lee, and Jie Xiong. 2020. FM-track: pushing the limits of contactless multi-target tracking using acoustic signals. In *Proceedings of the 18th Conference on Embedded Networked Sensor Systems*. 150–163.

[23] Shuai Li, Junchen Guo, Rui Xi, Chunhui Duan, Zhengang Zhai, and Yuan He. 2021. Pedestrian trajectory based calibration for multi-radar network. In *INFOCOM WKSHPS (2021)*.

[24] Xiang Li, Daqing Zhang, Qin Lv, Jie Xiong, Shengjie Li, Yue Zhang, and Hong Mei. 2017. IndoTrack: Device-free indoor human tracking with commodity Wi-Fi. *ACM IMWUT 2017* 1, 3 (2017), 1–22.

[25] Novelda LLC. [n. d.]. X4M03 Radar Development Kit. https://www.xethru.com/xethru-development-platform.html

[26] Chengwen Luo, Hande Hong, and Mun Choon Chan. 2014. PiLoc: A self-calibrating participatory indoor localization system. In *IPSN-14*. IEEE, 143–153.

[27] Emiliano Miluzzo, Nicholas D Lane, Andrew T Campbell, and Reza Olfati-Saber. 2008. CaliBree: A self-calibration system for mobile sensor networks. In *International Conference on Distributed Computing in Sensor Systems*. Springer, 314–331.

[28] Mostafa Mirshekari, Shijia Pan, Jonathon Fagert, Eve M Schooler, Pei Zhang, and Hae Young Noh. 2018. Occupant localization using footstep-induced structural vibration. *Mechanical Systems and Signal Processing* 112 (2018), 77–97.

[29] Caner Ozdemir. 2012. *Inverse synthetic aperture radar imaging with MATLAB algorithms*. Vol. 210. John Wiley & Sons.

[30] Shijia Pan, Tong Yu, Mostafa Mirshekari, Jonathon Fagert, Amelie Bonde, Ole J Mengshoel, Hae Young Noh, and Pei Zhang. 2017. Footprintid: Indoor pedestrian identification through ambient structural vibration sensing. *Proceedings of ACM IMWUT* 1, 3 (2017), 1–31.

[31] Nissanka B Priyantha, Hari Balakrishnan, Erik Demaine, and Seth Teller. 2003. Anchor-free distributed localization in sensor networks. In *the 1st Sensys*.

[32] Kun Qian, Chenshu Wu, Yi Zhang, Guidong Zhang, Zheng Yang, and Yunhao Liu. 2018. Widar2. 0: Passive human tracking with a single Wi-Fi link. In *MobiSys*.

[33] Anish Shastri, Marco Canil, Jacopo Pegoraro, Paolo Casari, and Michele Rossi. 2022. mmSCALE: Self-Calibration of mmWave Radar Networks from Human Movement Trajectories. In *RadarConf22*. IEEE, 1–6.

[34] Jamie Shotton, Andrew Fitzgibbon, Mat Cook, Toby Sharp, Mark Finocchio, Richard Moore, Alex Kipman, and Andrew Blake. 2011. Real-time human pose recognition in parts from single depth images. In *CVPR 2011*. Ieee, 1297–1304.

[35] Weiguo Wang, Jinming Li, Yuan He, and Yunhao Liu. 2020. Symphony: localizing multiple acoustic sources with a single microphone array. In *Proceedings of the 18th Conference on Embedded Networked Sensor Systems*. 82–94.

[36] Yizhou Wang, Zhongyu Jiang, Xiangyu Gao, Jenq-Neng Hwang, Guanbin Xing, and Hui Liu. 2021. Rodnet: Radar object detection using cross-modal supervision. In *IEEE/CVF WACV*. 504–513.

[37] Yaxiong Xie, Jie Xiong, Mo Li, and Kyle Jamieson. 2019. mD-Track: Leveraging Multi-Dimensionality for Passive Indoor Wi-Fi Tracking. In *The 25th Annual International Conference on Mobile Computing and Networking*. ACM, 1–16.

[38] Zongxing Xie, Bing Zhou, Xi Cheng, Elinor Schoenfeld, and Fan Ye. 2021. VitalHub: Robust, Non-Touch Multi-User Vital Signs Monitoring using Depth Camera-Aided UWB. In *2021 IEEE 9th International Conference on Healthcare Informatics*.

[39] Zongxing Xie, Bing Zhou, Xi Cheng, Elinor Schoenfeld, and Fan Ye. 2022. Passive and Context-Aware In-Home Vital Signs Monitoring Using Co-Located UWB-Depth Sensor Fusion. *ACM Transactions on Computing for Healthcare* (2022).

[40] Hao Xue, Lin Ma, and Xuezhi Tan. 2016. A fast visual map building method using video stream for visual-based indoor localization. In *IWCMC 2016*.

[41] Cemin Zhang, Michael Kuhn, Brandon Merkl, Aly E Fathy, and Mohamed Mahfouz. 2006. Accurate UWB indoor localization system utilizing time difference of arrival approach. In *2006 IEEE radio and wireless symposium*. IEEE, 515–518.

[42] Pei Zhang, Shijia Pan, Mostafa Mirshekari, Jonathon Fagert, and Hae Young Noh. 2019. Structures as sensors: Indirect sensing for inferring users and environments. *Computer* 52, 10 (2019), 84–88.

[43] Yonghao Zhao, Wai-Choong Wong, Tianyi Feng, and Hari Krishna Garg. 2019. Calibration-free indoor positioning using crowdsourced data and multidimensional scaling. *IEEE Transactions on Wireless Communications* 19, 3 (2019).